Smart Materials

DOI: 10.1002/ange.201202823

Patterned Superomniphobic–Superomniphilic Surfaces: Templates for Site-Selective Self-Assembly**

*Sai P. R. Kobaku, Arun K. Kota, Duck Hyun Lee, Joseph M. Mabry, and Anish Tuteja**

Superhydrophobic surfaces display apparent contact angles greater than 150° and low contact angle hysteresis with water, while superoleophobic surfaces display apparent contact angles greater than 150° and low contact angle hysteresis with low-surface-tension liquids such as oils and alcohols.[1] Superomniphobic surfaces display both superhydrophobicity and superoleophobicity. Similarly, superomniphilic surfaces display both superhydrophilicity and superoleophilicity, that is, apparent contact angles of about 0° with both water and low-surface-tension liquids.[2] Patterned surfaces containing well-defined domains that display both these extreme wetting properties have many potential applications in fog harvesting and liquid transport,[3] microchannels and microreactors,[4] enhanced condensation[5] and boiling[6] heat transfer, and the directed growth of thin films.[7] Further, such surfaces can also serve as templates for the wettability-driven self-assembly of liquids,[4] micro- or nanoparticles,[8] and DNA.[9] However, the majority of patterned surfaces developed thus far exhibit extreme wettability contrast only with high-surface-tension liquids such as water (surface tension, $\gamma_{lv} = 72.1\ mN\,m^{-1}$), thereby limiting the applications of such surfaces mostly to surfactant-free aqueous systems.[4–9]

To expand the application range to nonaqueous systems, especially those with low-surface-tension liquids such as oils (e.g., heptane, $\gamma_{lv} = 20.1\ mN\,m^{-1}$) and alcohols (e.g., methanol, $\gamma_{lv} = 22.5\ mN\,m^{-1}$), it is crucial to develop patterned superomniphobic–superomniphilic surfaces. While there have been a few reports on switchable superoleophobic–superoleophilic surfaces,[10] there are currently no reports on either superoleophobic or superomniphobic surfaces that are patterned with regular, well-defined superomniphilic domains (or vice-versa). Recent work[1,11] has explained how re-entrant surface texture, in conjunction with surface chemistry and roughness, can be used to design superomniphobic surfaces. In this work, we report a simple, fast, and practical methodology to develop patterned superomniphobic–superomniphilic surfaces that exhibit stark contrast in wettability with a wide range of polar and nonpolar liquids. Using these surfaces, we demonstrate the site-selective self-assembly of heptane upon dipping and spraying on textured surfaces, site-selective condensation and boiling with low-surface-tension liquids, and site-selective self-assembly of both polymers and microparticles.

When a liquid comes in contact with a textured surface, it adopts either the fully wetted Wenzel[12] state or the Cassie–Baxter[13] state, which supports a composite solid–liquid–air interface. The Cassie–Baxter state promotes high apparent contact angles (θ^*) and low contact angle hysteresis.[14] Development of superomniphobic surfaces requires the design of substrates that promote the formation of the Cassie–Baxter state with both water and low-surface-tension liquids. In recent work,[1] two dimensionless design parameters, spacing ratio D^* and robustness factor A^*, were discussed for the systematic design of superomniphobic surfaces. D^* is a measure of the air trapped underneath a liquid droplet in the Cassie–Baxter state. For textured substrates composed of discrete spherical particles (such as those considered here), $D^* = [(R+D)/R]^2$, where R is the radius of the spherical particle and D is half the inter-particle spacing. The Cassie–Baxter relationship can be written in terms of D^* as Equation (1).[1]

$$\cos\theta^* = -1 + \frac{1}{D^*}\left[\frac{\pi}{2\sqrt{3}}(1+\cos\theta)^2\right] \quad (1)$$

Here, θ is the Young's contact angle.[15] Higher values of D^* result in higher apparent contact angles [see Eq. (1)]. The robustness factor A^* represents the ratio between the breakthrough pressure $P_{breakthrough}$ required to force the transition from the nonwetting Cassie–Baxter state to the fully wetted Wenzel state and a characteristic reference pressure, P_{ref}, given as $P_{ref} = 2\gamma_{lv}/l_{cap}$, where $l_{cap} = \sqrt{\gamma_{lv}/\rho g}$ is the capillary length (here ρ is the liquid density and g is the acceleration because of gravity). This reference pressure P_{ref} is near the minimum possible pressure difference across the composite interface for millimetric sized or larger liquid droplets (or puddles) on extremely nonwetting textured surfaces.[1] For textured substrates with discrete spherical particles, the robustness factor A^* is given by Equation (2).[1]

[*] S. P. R. Kobaku, Prof. A. Tuteja
Department of Macromolecular Science and Engineering
University of Michigan
Ann Arbor, MI 48109 (USA)
E-mail: atuteja@umich.edu
Dr. A. K. Kota, Dr. D. H. Lee, Prof. A. Tuteja
Department of Materials Science and Engineering
University of Michigan
Ann Arbor, MI 48109 (USA)
Dr. J. M. Mabry
Rocket Propulsion Division
Air Force Research Laboratory
Edwards Air Force Base, CA 93524 (USA)

[**] We thank Dr. Charles Y-C. Lee and the Air Force Office of Scientific Research (AFOSR) for financial support under grant numbers FA9550-11-1-0017 and LRIR-12RZ03COR. We also thank the Department of Materials Science and Engineering and the University of Michigan for financial support.

Supporting information for this article is available on the WWW under http://dx.doi.org/10.1002/anie.201202823.

$$A^* = \frac{P_{breakthrough}}{P_{ref}} = \frac{2\pi l_{cap}}{R(2\sqrt{3}D^* - \pi)} \frac{(1-\cos\theta)}{(\sqrt{D^*} - 1 + 2\sin\theta)} \quad (2)$$

Any surface with $A^* \gg 1$ indicates the formation of a robust composite interface with high breakthrough pressures, whereas surfaces with $A^* < 1$ cannot form a stable composite interface, causing the liquid to penetrate the textured surface.

In this work, we fabricated superomniphobic surfaces by electrospinning solutions of 50 wt% 1H,1H,2H,2H-heptadecafluorodecyl polyhedral oligomeric silsequioxane (fluorodecyl POSS)[1] and poly(methyl methacrylate) (PMMA) in Asahiklin AK-225 (see section 1 in the Supporting Information). The highly porous, re-entrant, bead morphology of the electrospun surfaces ($D^* = 15.9$, see Figure 1a and section 1 in the Supporting Information) and the low surface energy of 50 wt% fluorodecyl POSS and PMMA blend ($\gamma_{sv} = 11.1\ mN\,m^{-1}$, see section 2 in the Supporting Information) lead to superomniphobicity.[1] The surfaces display a high robustness factor, high advancing contact angle (see Figure 1b), and low contact angle hysteresis for water ($A^* = 16.2$, $\theta^*_{adv} = 162°$ and $\Delta\theta^* = 2°$), as well as, for various low-surface-tension liquids (see section 3 in the Supporting Information), such as heptane ($A^* = 3.4$, $\theta^*_{adv} = 151°$, and $\Delta\theta^* = 10°$). When these superomniphobic surfaces are exposed to O_2 plasma, they turn superomniphilic, that is, $\theta^*_{adv} = \theta^*_{rec} \approx 0°$ for both water and heptane (see Figure 1b). These contact angles remain unchanged with time (see section 4 in the Supporting Information). The morphology of the electrospun beads also remains unaffected after O_2 plasma treatment (see Figure 1a). O_2 plasma treatment results in oxygen enrichment and simultaneous defluorination of the surface as indicated in the XPS spectrum by the change in intensities for the oxygen 1s and fluorine 1s peaks (see Figure 1c and section 5 in the Supporting Information) and the -CF_2 and -CF_3 groups in the high-resolution carbon 1s (see Figure 1d) XPS spectrum. The surface is likely defluorinated because of the degradation of the fluorinated end groups in fluorodecyl POSS.[16] The change in surface chemistry and consequently the change in surface energy (increased to $\gamma_{sv} = 67.8\ mN\,m^{-1}$, see section 2 in the Supporting Information) upon O_2 plasma treatment are also confirmed by contact angle measurements on nontextured surfaces spin-coated with 50 wt% fluorodecyl POSS and PMMA blend. The contact angles for water decreased from $\theta_{adv} = 123°$, $\theta_{rec} = 110°$ to $\theta_{adv} = 20°$, $\theta_{rec} = 0°$, while those for heptane decreased from $\theta_{adv} = 61°$, $\theta_{rec} = 38°$ to $\theta_{adv} = 10°$, $\theta_{rec} = 0°$ upon O_2 plasma treatment. This results in extremely low robustness factors, $A^* = 0.8$ for water and $A^* = 0.1$ for heptane on the electrospun bead surface, which explain the superomniphilic behavior after O_2 plasma treatment.

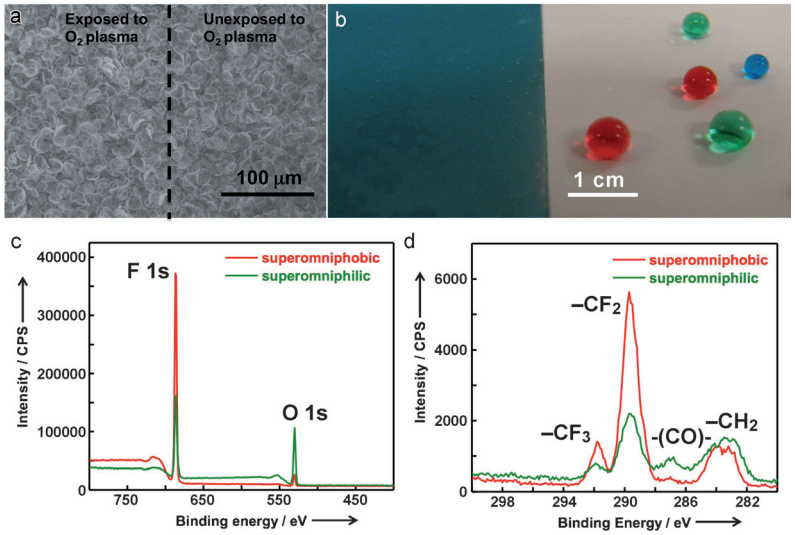

Figure 1. a) A SEM image showing electrospun bead morphology at the interface of the areas exposed and not exposed to O_2 plasma. This image indicates that there is no change in the bead morphology after O_2 plasma treatment. b) An electrospun bead surface (composed of 50 wt% fluorodecyl POSS and PMMA) that was exposed to O_2 plasma on the left (superomniphilic) and not exposed to O_2 plasma on the right (superomniphobic). Water (dyed blue) completely wets the superomniphilic region, but shows a high contact angle on the superomniphobic region. Heptane (dyed red) and methanol (dyed green) also show high contact angles on the superomniphobic region. The reflective surface visible underneath the droplets on the superomniphobic surface indicates the presence of microscopic pockets of air because of the formation of a composite interface. c,d) XPS spectra for the superomniphobic surface and the superomniphilic surface, respectively. The elemental peaks in (c) correspond to fluorine and oxygen, while the high-resolution carbon 1s peaks in (d) correspond to the different carbon moieties present on the surface.

By using a perforated stainless steel mask possessing the desired geometry (see section 1 in the Supporting Information) or a photoresist mask (fabricated using the novel photoresist mask transfer (PRMT) method developed herein; see section 6 in the Supporting Information) during O_2 plasma treatment, we fabricated superomniphilic domains on superomniphobic surfaces. Our PRMT method, based on photolithography, is extremely versatile because it allows us to fabricate patterned superomniphilic–superomniphobic surfaces with different sizes and shapes easily. When such a patterned surface (see Figure 2a) is dipped in heptane (dyed red), heptane selectively wets the superomniphilic domains because of the extreme wettability contrast, resulting in the self-assembly of heptane droplets within the superomniphilic patterns (see Figure 2b and Movie S1). This self-assembly is also assisted by the low contact angle hysteresis of heptane ($\Delta\theta^* = 10°$, roll-off angle $\omega \approx 7°$) on the superomniphobic regions. Similar self-assembly of heptane droplets is also obtained by spraying heptane on the patterned surfaces (see Movie S2). Figure 2c–f shows the site-selective self-assembly of heptane droplets on superomniphobic surfaces patterned with either circular or striped superomniphilic domains. Such self-assembled organic liquids can serve as surface-directed microchannels and microreactor arrays for liquid-phase reactions.[4,17]

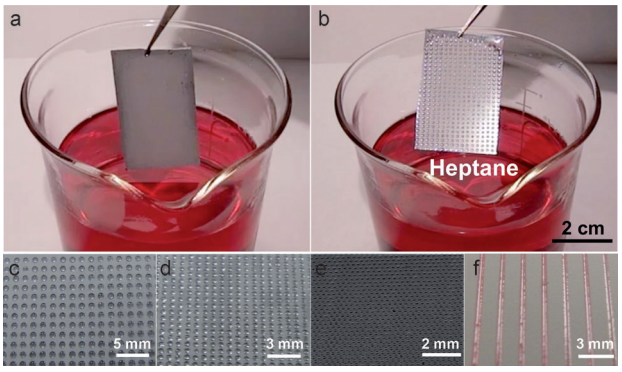

Figure 2. a) A superomniphobic surface patterned with superomniphilic domains before dipping in a beaker filled with heptane (dyed red). b) Site-selective self-assembly of heptane droplets within the superomniphilic domains after dipping in heptane. c–f) Site-selective self-assembly obtained by spraying heptane on patterned surfaces with superomniphilic domains. Surfaces in (c, d, and e) have circular superomniphilic domains of diameters 800, 510, and 150 μm, respectively. They were fabricated using stainless steel masks. The surface in (f) has striped superomniphilic domains of width 500 μm. It was fabricated using our PRMT method.

It has been recently demonstrated that superhydrophobic surfaces with superhydrophilic domains enhance condensation heat transfer,[5] while superhydrophilic surfaces with superhydrophobic domains enhance boiling heat transfer.[6] However, such surfaces can enhance heat transfer only when water is the heat transfer fluid. Many heat transfer operations (e.g., refrigeration and distillation) involve nonaqueous liquids with low surface tension. Here, we demonstrate the applicability of our patterned superomniphobic–superomniphilic surfaces in potentially enhancing condensation and boiling heat transfer even with low-surface-tension liquids. First, we exposed our superomniphobic surface patterned with superomniphilic domains to heptane vapors (by heating a reservoir of heptane at 50 °C). Figure 3 a and b illustrates

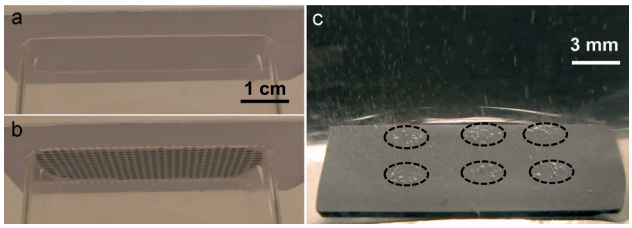

Figure 3. a,b) Superomniphobic surface patterned with superomniphilic domains before and after exposure, respectively, to heptane vapors. The site-selective condensation of heptane vapors within the superomniphilic domains is evident in (b). c) Superomniphilic surface patterned with superomniphobic domains immersed in boiling methanol. It is evident that the methanol vapor bubbles preferentially nucleate on the superomniphobic domains (black dashed circles).

how heptane vapors preferentially condense on, and wet, the superomniphilic domains (also see Movie S3). This is because of the strong dependence of heterogeneous nucleation on the Young's contact angle of the surface.[5] We estimate that the nucleation rate for heptane condensation on the superomniphilic regions of the surface is about five orders of magnitude higher than that on the superomniphobic regions, based on Volmer's classical nucleation theory (see section 7 in the Supporting Information).[18] Note that this site-selective condensation in superomniphilic domains is observed even though the Young's contact angle for heptane on both the superomniphobic domains ($\theta_{adv} = 61°$) and the superomniphilic domains ($\theta_{adv} = 10°$) is less than 90°, that is, both the domains are inherently oleophilic.[1]

In our control experiments, we observed a similar site-selective condensation of heptane vapors on nontextured (smooth) surfaces with patterned wettability. However, similar to previous reports,[5] we observed that the patterned nontextured surfaces do not promote roll-off of the condensed droplets like the patterned superomniphobic surfaces. Surfaces that provide high nucleation rates for condensation (superomniphilic domains), while also providing efficient roll-off of the condensed droplets, are important as they promote drop-wise condensation over film-wise condensation.[5]

We also immersed our superomniphilic surface patterned with superomniphobic domains in boiling methanol at 65 °C (the boiling point for methanol). Figure 3 c illustrates that the methanol vapor bubbles preferentially nucleate on the superomniphobic domains (also see Movie S4). Surfaces that are not easily wetted by the boiling liquid (i.e., surfaces with low surface energy) exhibit a high value for the boiling heat transfer coefficient (HTC) because they facilitate bubble nucleation. In control experiments, we observed that low surface energy non-textured surfaces facilitate bubble nucleation. However, as reported previously,[6] the cavities (air trapped) in low surface energy textured surfaces provide additional sites for nucleation of vapor bubbles. Consequently, superomniphobic surfaces are expected to yield high values for the HTC,[6] even for low-surface-tension heat-transfer liquids. As the heat flux increases, the rate of nucleation of bubbles increases and at the critical heat flux (CHF), the over-crowded bubbles coalesce to form a continuous vapor film between the heating surface and the boiling liquid.[6] This vapor film possesses a high thermal resistance and acts as a barrier to heat transfer. Thus, it is desirable to increase the CHF.[6] High CHF can be achieved by using surfaces that are easily wetted by the boiling liquid (i.e., surfaces with high surface energy).[6] Consequently, superomniphilic surfaces are expected to yield a high CHF. Surfaces that provide high nucleation rates for boiling liquids (superomniphobic domains), while also efficiently preventing the formation of a continuous vapor film (superomniphilic surface), even with low-surface-tension liquid systems, such as those developed here, are therefore of significant importance for simultaneously increasing both HTC and CHF. Our patterned surfaces provide an avenue for systematically varying the domain size and the interdomain spacing in order to study enhanced condensation and boiling heat transfer[5–6] with both high- and low-surface-tension liquids.

We have also used our superomniphobic surfaces patterned with superomniphilic domains as templates for wettability-driven site-selective self-assembly of microparticles and polymers. When a dispersion of UV fluorescent green microspheres in water is sprayed on the patterned surface,

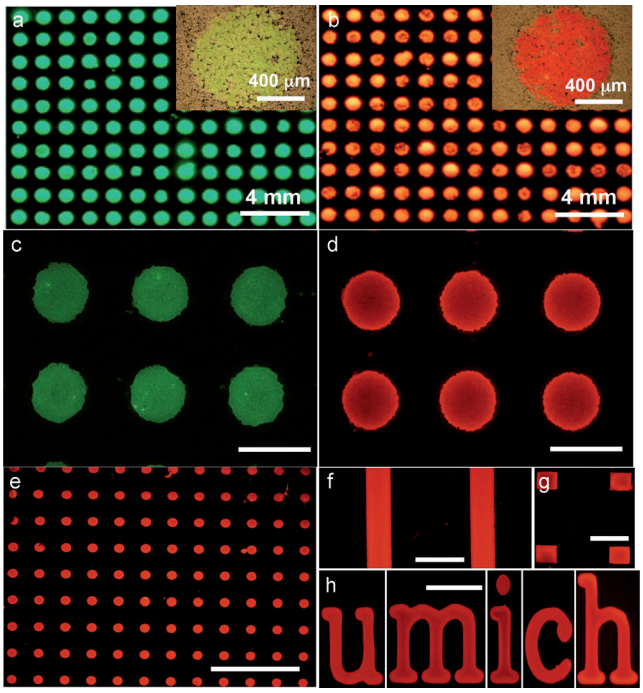

Figure 4. a,b) Site-selective self-assembly of UV fluorescent green microspheres dispersed in water and UV fluorescent red microspheres dispersed in heptane, respectively. The pictures in (a) and (b) were obtained under a 365 nm UV lamp and the corresponding insets show higher magnification optical microscope images. c) Site-selective self-assembly of PVP dissolved in water using 800 μm diameter circular superomniphilic domains. d,e) Site-selective self-assembly of PIB dissolved in heptane using 800 and 100 μm diameter circular superomniphilic domains, respectively. f–h) Site-selective self-assembly of PIB using superomniphilic domains of noncircular shapes. The pictures in (c–h) were obtained using fluorescent microscopy and the scale bars represent 1 mm.

water droplets and consequently the microspheres are confined within the superomniphilic domains. After the water dries, the microspheres are deposited within the superomniphilic domain (see inset in Figure 4a), resulting in site-selective self-assembly of microspheres (see Figure 4a). Similarly, we obtained site-selective self-assembly of UV fluorescent red microspheres in heptane (see Figure 4b). We also obtained site-selective self-assembly of poly(vinyl pyrrolidone) (PVP) films (see Figure 4c) and poly(isobutylene) (PIB) films (see Figure 4d) by spraying solutions of PVP in water and PIB in heptane, respectively. We also obtained PIB films of different sizes and shapes using our PRMT methodology (see Figure 4e–h and section 8 in the Supporting Information). Thus, our methodology offers a simple route to make precisely tailored arrays of microparticles and polymer films of different sizes and shapes on textured surfaces using both high- and low-surface-tension liquids. Such precise control over the site-selective self-assembly of particles and films can be useful in developing electronic and optical devices,[8] patterned assembly of cells, and growth of well-defined thin films and nanostructures (3D assembly).[7]

In conclusion, we have demonstrated a facile methodology to create patterned superomniphobic–superomniphilic surfaces. Using our patterned surfaces, we have obtained site-selective self-assembly of heptane droplets through dipping and spraying. Such self-assembled organic liquids can serve as microreactor arrays for liquid-phase reactions. We have also demonstrated the preferential condensation of heptane within patterned superomniphilic domains and preferential boiling of methanol on patterned superomniphobic domains. Such surfaces provide an avenue to study enhanced condensation and boiling heat transfer with both high- and low-surface-tension liquids. We have also used our superomniphobic surfaces patterned with superomniphilic domains as templates for wettability-driven site-selective self-assembly of microparticles and polymers.

Received: April 12, 2012
Revised: August 10, 2012
Published online: August 31, 2012

Keywords: materials science · self-assembly · surface chemistry · wettability

[1] a) A. Tuteja, W. Choi, J. M. Mabry, G. H. McKinley, R. E. Cohen, *Proc. Natl. Acad. Sci. USA* **2008**, *105*, 18200; b) A. Tuteja, W. Choi, M. Ma, J. M. Mabry, S. A. Mazzella, G. C. Rutledge, G. H. McKinley, R. E. Cohen, *Science* **2007**, *318*, 1618; c) A. Tuteja, W. Choi, G. H. McKinley, R. E. Cohen, M. F. Rubner, *MRS Bull.* **2008**, *33*, 752; d) S. S. Chhatre, W. Choi, A. Tuteja, K. C. Park, J. M. Mabry, G. H. McKinley, R. E. Cohen, *Langmuir* **2010**, *26*, 4027.

[2] K. Koch, I. C. Blecher, G. Koenig, S. Kehraus, W. Barthlott, *Funct. Plant Biol.* **2009**, *36*, 339.

[3] a) L. Zhai, M. C. Berg, F. C. Cebeci, Y. Kim, J. M. Milwid, M. F. Rubner, R. E. Cohen, *Nano Lett.* **2006**, *6*, 1213; b) Y. Zheng, H. Bai, Z. Huang, X. Tian, F.-Q. Nie, Y. Zhao, J. Zhai, L. Jiang, *Nature* **2010**, *463*, 640.

[4] a) D. A. Bruzewicz, M. Reches, G. M. Whitesides, *Anal. Chem.* **2008**, *80*, 3387; b) E. Carrilho, A. W. Martinez, G. M. Whitesides, *Anal. Chem.* **2009**, *81*, 7091; c) D. Zahner, J. Abagat, F. Svec, J. M. J. Frechet, P. A. Levkin, *Adv. Mater.* **2011**, *23*, 3030; d) B. Zhao, J. S. Moore, D. J. Beebe, *Science* **2001**, *291*, 1023; e) G. Chitnis, Z. Ding, C.-L. Chang, C. A. Savran, B. Ziaie, *Lab Chip* **2011**, *11*, 1161; f) H. Gau, S. Herminghaus, P. Lenz, R. Lipowsky, *Science* **1999**, *283*, 46.

[5] a) K. K. Varanasi, M. Hsu, N. Bhate, W. Yang, T. Deng, *Appl. Phys. Lett.* **2009**, *95*, 094101; b) X. Chen, J. Wu, R. Ma, M. Hua, N. Koratkar, S. Yao, Z. Wang, *Adv. Funct. Mater.* **2011**, *21*, 4617; c) N. A. Patankar, *Soft Matter* **2010**, *6*, 1613.

[6] a) A. R. Betz, J. Xu, H. Qiu, D. Attinger, *Appl. Phys. Lett.* **2010**, *97*, 141909; b) A. R. Betz, J. R. Jenkins, C. J. Kim, D. Attinger, Ieee in *2011 IEEE 24th Intl. Conf. MEMS*, IEEE, New York, **2011**, pp. 1193; c) H. Jo, H. S. Ahn, S. Kane, M. H. Kim, *Int. J. Heat Mass Transfer* **2011**, *54*, 5643.

[7] a) T. Balgar, S. Franzka, E. Hasselbrink, N. Hartmann, *Appl. Phys. A* **2006**, *82*, 15; b) R. Maoz, S. R. Cohen, J. Sagiv, *Adv. Mater.* **1999**, *11*, 55; c) Y. Masuda, S. Ieda, K. Koumoto, *Langmuir* **2003**, *19*, 4415.

[8] a) Y. Masuda, K. Tomimoto, K. Koumoto, *Langmuir* **2003**, *19*, 5179; b) D. Qin, Y. N. Xia, B. Xu, H. Yang, C. Zhu, G. M. Whitesides, *Adv. Mater.* **1999**, *11*, 1433; c) D. Hohnholz, H. Okuzaki, A. G. MacDiarmid, *Adv. Funct. Mater.* **2005**, *15*, 51; d) L. Li, L. Jiang, W. Wang, C. Du, H. Fuchs, W. Hu, L. Chi, *Adv. Mater.* **2012**, *24*, 2159.

[9] S. D. Gillmor, A. J. Thiel, T. C. Strother, L. M. Smith, M. G. Lagally, *Langmuir* **2000**, *16*, 7223.

[10] a) J. Yang, Z. Zhang, X. Men, X. Xu, X. Zhu, X. Zhou, Q. Xue, *J. Colloid Interface Sci.* **2012**, *366*, 191; b) M. Zhang, T. Zhang, T. Cui, *Langmuir* **2011**, *27*, 9295; c) J. Zimmermann, M. Rabe, G. R. J. Artus, S. Seeger, *Soft Matter* **2008**, *4*, 450; d) W. Choi, A. Tuteja, S. Chhatre, J. M. Mabry, R. E. Cohen, G. H. McKinley, *Adv. Mater.* **2009**, *21*, 2190.
[11] a) A. Ahuja, J. A. Taylor, V. Lifton, A. A. Sidorenko, T. R. Salamon, E. J. Lobaton, P. Kolodner, T. N. Krupenkin, *Langmuir* **2008**, *24*, 9; b) L. Cao, T. P. Price, M. Weiss, D. Gao, *Langmuir* **2008**, *24*, 1640; c) A. Marmur, *Langmuir* **2008**, *24*, 7573.
[12] R. N. Wenzel, *Ind. Eng. Chem.* **1936**, *28*, 988.
[13] A. B. D. Cassie, S. Baxter, *Trans. Faraday Soc.* **1944**, *40*, 546.
[14] a) W. Chen, A. Y. Fadeev, M. C. Hsieh, D. Oner, J. Youngblood, T. J. McCarthy, *Langmuir* **1999**, *15*, 3395; b) C. W. Extrand, *Langmuir* **2002**, *18*, 7991; c) A. Lafuma, D. Quere, *Nat. Mater.* **2003**, *2*, 457.
[15] T. Young, *Philos. Trans. R. Soc. London* **1805**, *95*, 65.
[16] a) X. Li, J. Tian, T. Nguyen, W. Shen, *Anal. Chem.* **2008**, *80*, 9131; b) X. Zhu, Z. Zhang, X. Xu, X. Men, J. Yang, X. Zhou, Q. Xue, *Langmuir* **2011**, *27*, 14508.
[17] a) B. Wang, Q. H. Zhao, F. Wang, C. Y. Gao, *Angew. Chem.* **2006**, *118*, 1590; *Angew. Chem. Int. Ed.* **2006**, *45*, 1560; b) Z. Wang, H. Shang, G. U. Lee, *Langmuir* **2006**, *22*, 6723.
[18] a) R. A. Sigsbee, *Nucleation* (Ed.: A. C. Zettlemoyer), Marcel Dekker, New York, **1969**; b) M. Volmer, *Kinetik der Phasenbildung*, Steinkopff, Dresden, **1939**.

